Note
Carbon Letters Vol. 24, 111-114 (2017)

The electrical and heating properties of copper-incorporated graphite fibers fabricated using different ultrasonication techniques

Kyeong Min Lee[1], Min-Ji Kim[1], Hanjoo Jo[1], Sang Young Yeo[2] and Young-Seak Lee[1,♠]

[1]Department of Chemical Engineering and Applied Chemistry, Chungnam National University, Daejeon 34134, Korea
[2]Korea Institute of Industrial Technology (KITECH), Ansan 15588, Korea

Article Info

Received 11 March 2017
Accepted 4 July 2017

♠Corresponding Author
E-mail: youngslee@cnu.ac.kr
Tel: +82-42-821-7007

Open Access

DOI: http://dx.doi.org/10.5714/CL.2017.24.111

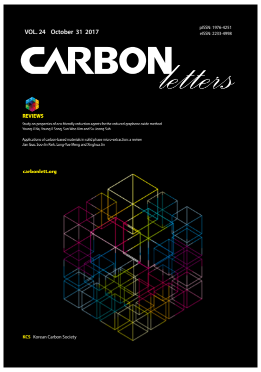

http://carbonlett.org

pISSN: 1976-4251
eISSN: 2233-4998

Electrical energy can be converted into heat energy through ohmic joule heating. Metallic materials are typically used in electrical heating elements because of their great electrical conductivity. However, metallic materials have several weaknesses, such as corrosion susceptibility, heavy weight, high manufacturing costs, and electromagnetic wave emissions [1,2]. To resolve these problems, carbon materials with good electrical conductivity, such as carbon fibers, graphite fibers, carbon nanotubes, and carbon black, have been examined as heating materials [3,4]. Among these carbon materials, graphite fibers possess many advantages compared to carbon fibers such as good mechanical and electrical properties, excellent chemical stability, high thermal conductivity, and so on [5-7]. However, the electrical conductivity of graphite fibers is much lower than that of copper, which is too low to improve the heating properties. Therefore, metal-incorporated graphite fibers have been considered as attractive materials to achieve improved heating properties [8,9]. Metal can be incorporated into carbon structures using several different methods, such as electrodeposition, electroless deposition, doping, and impregnation. Among these methods, impregnation by stirring in a metal solution is a simple, easy, and cost-effective method, but this method incorporates less metal into the structure than that of other methods [10,11]. To overcome this limitation, ultrasonication has been used to impregnate metal atoms in a solution, which can attach more metal atoms on the surface of supporters than that of previous impregnation methods because it provides more opportunities for reactions between supporters and metal atoms. Moreover, when a solution is exposed to ultrasonication, high temperature and pressure fields accelerating the chemical reaction may be produced at the centers of the generated bubbles in a solution. Therefore, ultrasonication treatment has become probably the most widely used and effective mechanical technique [12].

We developed a new method to introduce copper onto graphite fibers using both bath and tip ultrasonication. Additionally, we determined the effect of copper impregnation using different ultrasonication techniques on the copper-incorporated morphology and improved the electrical and heating properties of the graphite fibers. The graphite fibers used in this study were obtained from the Nippon Graphite Fiber Corp. (Japan), and the average diameter of the fibers was approximately 10 μm. First, 0.1 g of the fibers were immersed in 50 g of 0.1 M $CuSO_4$ solution and then treated by bath and tip ultrasonication for 20 min at room temperature. Next, the treated fibers were washed with distilled water and dried at 80°C for 12 h. The prepared samples were labeled according to the copper impregnation conditions as B20-GF and T20-GF, where the letters and numbers refer to the method of ultrasonication and the treatment time, respectively. R-GF refers to the raw graphite fibers. The bath and tip ultrasonication instruments used in this study were a Powersonic 405 ultrasonic cleaner from Hwashin Technology (Korea) and a VC-505 ultrasonic processor from Sonics & Materials (USA), which had generators with 400 and 500 W outputs, respectively. For tip ultrasonication, a titanium-tipped horn with an 11 mm-diameter tip was directly placed in the solution.

The surface morphology of the treated fibers was observed by scanning electron microscopy (SEM) with a Hitachi S-5500 microscope (Japan). Energy dispersive spectroscopy (EDS) was performed to confirm the copper using the same equipment. The amount of cop-

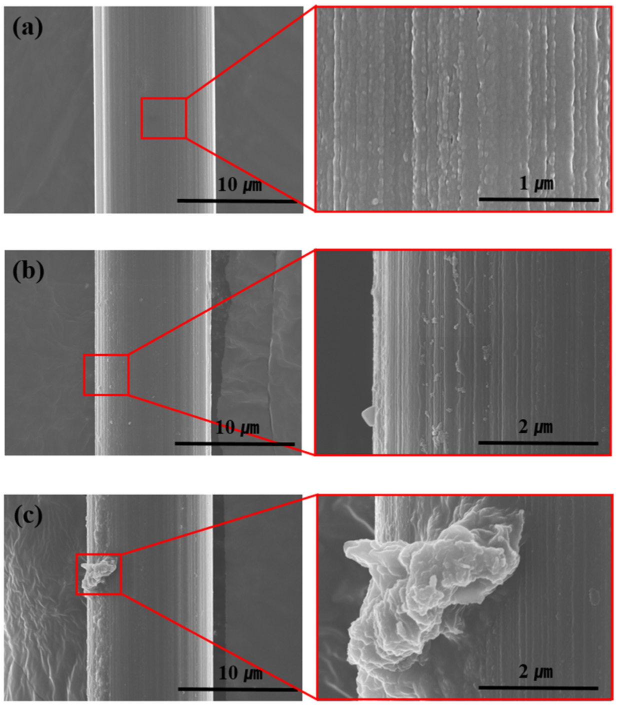

Fig. 1. Scanning electron microscopy images of the treated graphite fibers (GF): (a) R-GF, (b) B20-GF, and (c) T20-GF.

per on the treated fibers was determined by thermogravimetric analysis (TGA). TGA scans were recorded at 10°C/min from 25 to 870°C in an air atmosphere. In addition, the electrical resistance of the fibers exposed to air was measured on an electrometer (Keithley 6514) using only a strand of the treated fiber, of which the two ends of the sample were attached by silver paste and clamped on both sides. The sample size was 35 mm in length, and we calculated the average specific resistance. The heating properties were estimated with a thermographic camera at 25°C to observe the surface temperature of the treated fiber with the applied voltage.

Fig. 1 shows the SEM image of the raw and treated graphite fibers. As shown in Fig. 1a, the raw graphite fiber has a smooth surface. The graphite fibers treated by bath ultrasonication (Fig. 1b) revealed that the copper attached onto the graphite fibers due to the self-catalytic effect of copper growth [13,14]. When using tip ultrasonication, as shown in Fig. 1c, a large amount of copper particles was introduced onto the graphite fibers compared with the amount resulting from the bath ultrasonication. This is because not only the power of the tip ultrasonication is higher than that of the bath ultrasonication, but also, the tip was directly submerged in solution. Therefore, more energy was applied to introduce more copper in the tip ultrasonication [15-17]. As shown in Fig. 2, the EDS element mapping of the copper-incorporated graphite fibers shows the presence of the C, O and Cu. It can be confirmed that a larger amount of copper was introduced into the T20-GF than into the B20-GF. Moreover, because oxygen was observed to be near the copper particles, it is believed that the copper of B20-GF and T20-GF exist as copper oxides.

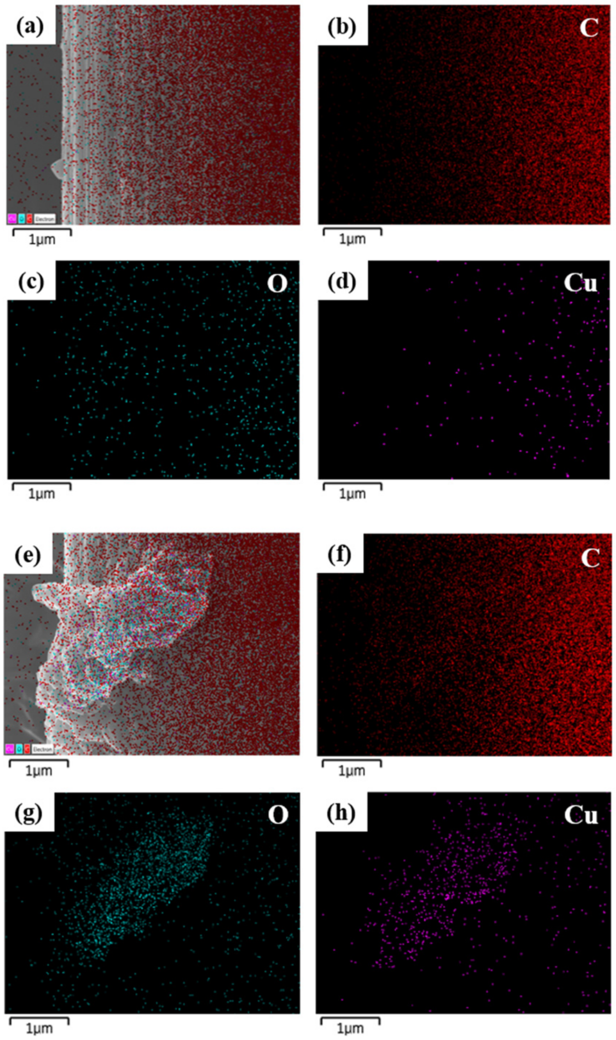

Fig. 2. C, O, and Cu element mapping of the copper-incorporated graphite fibers (GF). (a-d) B20-GF and (e-h) T20-GF.

TGA was conducted to calculate the amount of copper on the graphite fibers and to examine the thermal behavior of the treated graphite fibers [18,19]. As shown in Table 1 and Fig. 3, the thermal behavior of the treated graphite fibers was similar to that of the raw graphite fibers, exhibiting a 5% weight loss above approximately 700°C. The weight of the raw graphite fibers was 0% at approximately 865°C, which indicates that the graphite fibers had thermally decomposed. Additionally, B20-GF and T20-GF did not tend to increase in weight under 500°C in an air atmosphere. As mentioned in Fig. 2, these results are attributed to the attached particles on the B20-GF and T20-GF as a form of oxide.

The changes in the residue weight indicate the relative amount of copper introduced onto the graphite fibers according to the ultrasonication technique. The weight of copper introduced onto the T20-GF was approximately 3.5 times more than that of the B20-GF because of the higher energy of the tip ultrasonication compared with the bath ultrasonication.

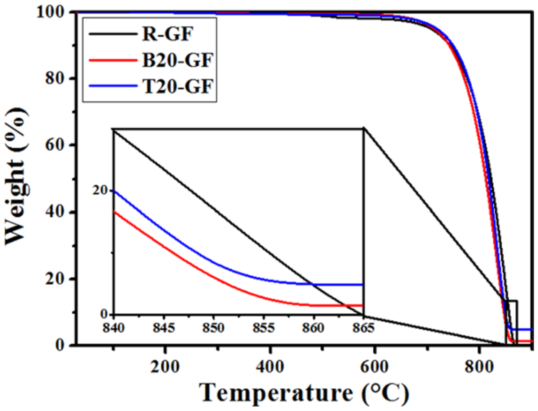

Fig. 3. Thermogravimetric analysis graph of the copper-incorporated graphite fibers (GF) based on the ultrasonication techniques.

The amount of copper introduced onto the treated graphite fibers influences the electrical conductivity, which determines the heating properties [20]. Table 1 also presents the average specific resistance and the calculated electrical conductivity of the treated graphite fibers. The introduction of copper onto the graphite fibers obviously improved the electrical conductivity [21]. The electrical conductivity of T20-GF was higher than that of B20-GF because of the amount of copper introduced (Table 1).

Fig. 4 shows the surface temperature of the samples at different levels of applied voltages (a) and electric power (b) in the range of 30–50 V and 0.2–1.6 W, respectively. The surface temperature of each sample was examined after 30 s at a voltage. The surface temperature of all the samples rapidly increased with the applied voltage. Additionally, the copper-incorporated graphite fibers exhibited a higher surface temperature than that of the raw graphite fibers at the same electric power. The maximum temperature of T20-GF at an applied power of 1.5 W and applied voltage of 50 V was 45.9°C. This increased temperature resulted from an increase in the electrical conductivity due to the amount of copper introduced onto the graphite fiber. Therefore, the electrical current of the treated graphite fibers increased at the same applied voltage, and the treated graphite fibers showed improved heating properties.

In conclusion, copper was effectively introduced onto graphite fibers with an easy and simple method using tip and bath ultrasonication techniques. The amount of copper on the graphite fibers treated with the tip ultrasonication was higher than that on the graphite fibers treated with bath ultrasonication. Therefore, tip ultrasonication is more effective at introducing copper onto graphite fibers compared to bath ultrasonication because tip ultrasonication can apply more energy than that of bath ultrasonication. Likewise, the graphite fibers treated by tip ultrasonication for 20 min showed improved electrical conductivity and heating properties, with the surface temperature reaching about 46°C with 1.5 W of applied electric power. Therefore, copper incorporation onto graphite fibers by tip ultrasonication can be successfully used to fabricate electrical heating materials with improved electrical conductivity and heating properties.

Conflict of Interest

No potential conflict of interest relevant to this article was reported.

Table 1. Thermogravimetric analysis results and electrical properties of the copper-incorporated graphite fibers

	Pyrolysis temperature (°C)		Final weight (%)	Average specific resistance (Ω cm)	Average electrical conductivity (S cm^{-1})
	Start (a 5% weight loss)	End			
R-GF	706	865	0	0.000699 (±0.000024)	1430.94
B20-GF	712	855	1.441	0.000682 (±0.000019)	1466.39
T20-GF	717	855	4.868	0.000662 (±0.000021)	1510.54

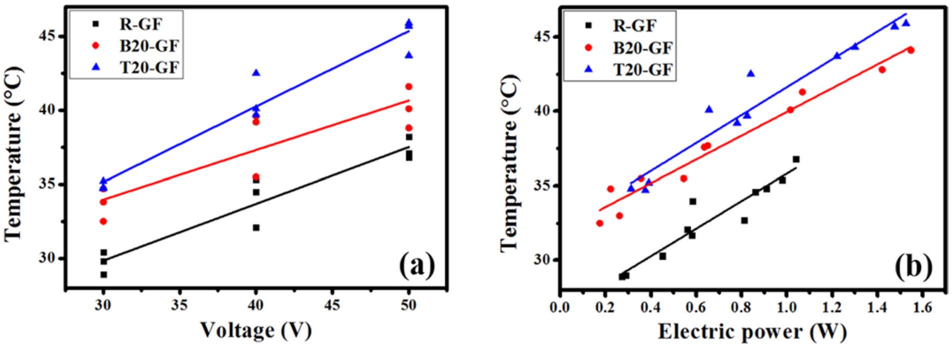

Fig. 4. Surface temperature of the copper-incorporated graphite fibers (GF) based on the ultrasonication techniques. (a) The relation of temperature and voltage and (b) the relation of temperature and electric power.

Acknowledgements

This work was supported by the Human Resources Program in Energy Technology of the Korea Institute of Energy Technology Evaluation and Planning (KETEP) which is supported by the Ministry of Trade, Industry & Energy, Republic of Korea (20164010201070).

References

[1] Tang P, Zhang R, Shi R, Bin Y. Synergetic effects of carbon nanotubes and carbon fibers on electrical and self-heating properties of high-density polyethylene composites. J Mater Sci, **50**, 1565 (2015). https://doi.org/10.1007/s10853-014-8716-z.

[2] Fosbury A, Wang S, Pin YF, Chung DDL. The interlaminar interface of a carbon fiber polymer-matrix composite as a resistance heating element. Compos Part A Appl Sci Manuf, **34**, 933 (2003). https://doi.org/10.1016/S1359-835X(03)00208-2.

[3] Kim GM, Yang BJ, Ryu GU, Lee HK. The electrically conductive carbon nanotube (CNT)/cement composites for accelerated curing and thermal cracking reduction. Compos Struct, **158**, 20 (2016). https://doi.org/10.1016/j.compstruct.2016.09.014.

[4] He Y, Yang R, Zhang H, Zhou D, Wang G. Volume or inside heating thermography using electromagnetic excitation for advanced composite materials. Int J Therm Sci, **111**, 41 (2017). https://doi.org/10.1016/j.ijthermalsci.2016.08.007.

[5] Park MS, Ko Y, Jung MJ, Lee YS. Stabilization of pitch-based carbon fibers accompanying electron beam irradiation and their mechanical properties. Carbon Lett, **16**, 121 (2015). https://doi.org/10.5714/CL.2015.16.2.121.

[6] Yang J, Nakabayashi K, Miyawaki J, Yoon SH. Preparation of isotropic pitch-based carbon fiber using hyper coal through co-carbonation with ethylene bottom oil. J Ind Eng Chem, **34**, 397 (2016). https://doi.org/10.1016/j.jiec.2015.11.026.

[7] Yu X, Han X, Zhao Z, Zhang J, Guo W, Pan C, Li A, Liu H, Wang ZL. Hierarchical TiO_2 nanowire/graphite fiber photoelectrocatalysis setup powered by a wind-driven nanogenerator: a highly efficient photoelectrocatalytic device entirely based on renewable energy. Nano Energy, **11**, 19 (2015). https://doi.org/10.1016/j.nanoen.2014.09.024.

[8] Xu C, Liu G, Chen H, Zhou R, Liu Y. Fabrication of conductive copper-coated glass fibers through electroless plating process. J Mater Sci Mater Electron, **25**, 2611 (2014). https://doi.org/10.1007/s10854-014-1919-x.

[9] Katwal R, Kaur H, Sharma G, Naushad M, Pathania D. Electrochemical synthesized copper oxide nanoparticles for enhanced photocatalytic and antimicrobial activity. J Ind Eng Chem, **31**, 173 (2015). https://doi.org/10.1016/j.jiec.2015.06.021.

[10] Kim JH, Kim KH, Park MS, Bae TS, Lee YS. Cu nanoparticle-embedded carbon foams with improved compressive strength and thermal conductivity. Carbon Lett, **17**, 65 (2016). https://doi.org/10.5714/CL.2016.17.1.065.

[11] Yuan E, Zhang K, Lu G, Mo Z, Tang Z. Synthesis and application of metal-containing ZSM-5 for the selective catalytic reduction of NO_x with NH_3. J Ind Eng Chem, **42**, 142 (2016). https://doi.org/10.1016/j.jiec.2016.07.030.

[12] Ruan B, Jacobi AM. Ultrasonication effects on thermal and rheological properties of carbon nanotube suspensions. Nanoscale Res Lett, **7**, 127 (2012). https://doi.org/10.1186/1556-276X-7-127.

[13] Festag G, Steinbrück A, Csáki A, Möller R, Fritzsche W. Single particle studies of the autocatalytic metal deposition onto surface-bound gold nanoparticles reveal a linear growth. Nanotechnology, **18**, 015502 (2006). https://doi.org/10.1088/0957-4484/18/1/015502.

[14] Chong SP, Ee YC, Chen Z, Law SB. Electroless copper seed layer deposition on tantalum nitride barrier film. Surf Coat Technol, **198**, 287 (2005). https://doi.org/10.1016/j.surfcoat.2004.10.086.

[15] Ghani SA, Hassan RH, Yaseen ST. The preparation, characterization, and catalytic activity of synthetic activated carbon supported cupric chloride in oxidation of iraqi naphtha. Energy Sources Part A Recovery Util Environ Eff, **34**, 1471 (2012). http://dx.doi.org/10.1080/15567036.2011.608775.

[16] Schrage C, Kaskel S. Flexible and transparent SWCNT electrodes for alternating current electroluminescence devices. ACS Appl Mater Interface, **8**, 1640 (2009). https://doi.org/10.1021/am9002588.

[17] Liao YH, Marietta-Tondin O, Liang Z, Zhang C, Wang B. Investigation of the dispersion process of SWNTs/SC-15 epoxy resin nanocomposites. Mater Sci Eng A, **385**, 175 (2004). https://doi.org/10.1016/j.msea.2004.06.031.

[18] Choi CH, Park SH, Woo SI. N-doped carbon prepared by pyrolysis of dicyandiamide with various $MeCl_2 \cdot xH_2O$ (Me = Co, Fe, and Ni) composites: effect of type and amount of metal seed on oxygen reduction reactions. Appl Catal B Environ, **119-120**, 123 (2012). https://doi.org/10.1016/j.apcatb.2012.02.031.

[19] Sahiiner N, Sagbas S. The use of poly(vinyl phosphonic acid) microgels for the preparation of inherently magnetic Co metal catalyst particles in hydrogen production. J Power Sources, **246**, 55 (2014). https://doi.org/10.1016/j.jpowsour.2013.07.043.

[20] Chien AT, Cho S, Joshi Y, Kumar S. Electrical conductivity and joule heating of polyacrylonitrile/carbon nanotube composite fibers. Polymer, **55**, 6896 (2014). https://doi.org/10.1016/j.polymer.2014.10.064.

[21] Zhang D, Ye L, Deng S, Zhang J, Tang Y, Chen Y. CF/EP composite laminates with carbon black and copper chloride for improved electrical conductivity and interlaminar fracture toughness. Compos Sci Technol, **72**, 412 (2012). https://doi.org/10.1016/j.compscitech.2011.12.002.